First absolute seasonal temperature estimates for greenhouse climate from clumped isotopes in bivalve shells

Niels J. de Winter[1,2]*, Inigo A. Müller[1], Ilja J. Kocken[1], Nicolas Thibault[3], Clemens V. Ullmann[4], Alex Farnsworth[5], Daniel J. Lunt[5], Philippe Claeys[2], Martin Ziegler[1]

[1]*Department of Earth Sciences, Faculty of Geosciences, Utrecht University, the Netherlands*

[2]*AMGC research group, Vrije Universiteit Brussel, Brussels, Belgium*

[3]*Faculty of Science, IGN, University of Copenhagen, Denmark*

[4]*Camborne School of Mines and Environment and Sustainability Institute, University of Exeter, UK*

[5]*School of Geographical Sciences, University of Bristol, UK.*

Corresponding author

ABSTRACT

The seasonal variability of sea surface temperatures plays a fundamental role in climate dynamics and species distribution. As such, it is essential to better understand seasonal variability in warm climates of the past. Previous reconstructions of seasonality in deep time are relatively unconstrained, relying on unsupported assumptions such as estimates of seawater composition and negligible seasonal bias. This work presents the first absolute seasonal temperature reconstructions based on clumped isotope measurements in bivalve shells which, critically, do not rely on these assumptions. Our new approach reconstructs highly precise mid-latitude (~50°N) monthly temperatures from individual oyster and rudist shells of the Campanian (78 million years ago) greenhouse period (15—27 °C seasonal range). Our analysis demonstrates that seasonal bias and previous assumptions about sea water oxygen isotope composition can lead to highly inaccurate temperature reconstructions, distorting our understanding of the behavior of greenhouse climates

and our ability to model them. Our results agree remarkably well with fully coupled climate model simulations showing greenhouse climates outside the tropics were warmer with higher seasonality than previously thought.

MAIN

Introduction

Temperature seasonality is a critical component governing the geographic distribution of modern flora and fauna while seasonal extremes were likely also of vital importance for the evolution and distribution of life over geological history[1]. The effects of greenhouse warming on seasonal variability in temperature and the hydrological cycle are still highly unconstrained and of considerable interest to allow quantification of projections of future climate and the ongoing biodiversity crisis[2,3]. Reconstructions of deep time (pre-Quaternary) greenhouse periods yield valuable insights into the dynamics of warm climates and the ecological response to forcing mechanisms such as rising atmospheric CO_2 levels[4,5]. Accurate reconstructions are imperative to evaluate climate model predictions under dissimilar climate states[6] in particular seasonal range for which there is little quantitative evidence to constrain climate model behavior. The warm, ice free Late Cretaceous period presents a valuable reference to assess seasonal variability in greenhouse climate[7,8].

Reconstructions based on stable oxygen isotope ratios ($\delta^{18}O_c$) in marine carbonates indicate that Late Cretaceous global mean sea surface temperatures (SST) were ~5-6°C warmer than today with a reduced latitudinal temperature gradient (an "equable climate"[9]) and the Late Cretaceous greenhouse is often regarded to have had limited temperature seasonality[7,10,11,12]. However, the reliability of past seasonal reconstructions is highly questionable as a result of methodological

unconstrained assumptions. This hampers our understanding of past warm climates and hinders accurate evaluation of climate models[13,14]. If a proxy is interpreted as representing annual mean conditions, but is in fact biased to a particular season, then this will limit our understanding of the behavior of greenhouse climates. This further leads to misinterpretation of model-data comparisons of past warm climates[15], and hinders the use of paleoclimate data for informing future climate predictions. In deep time, traditional temperature reconstructions based on fossil assemblages are highly uncertain or contentious, because studied fossil species may not have a modern close relative for proxy calibration[16]. In addition, ambient water oxygen isotope composition ($\delta^{18}O_{sw}$), which forms an important input parameter into the traditional carbonate $\delta^{18}O_c$ temperature proxy[17], remains poorly constrained across geological timescales[18,19]. These complications do not affect the carbonate clumped isotope (Δ_{47}) thermometer, which yields more accurate SST reconstructions[20,21]. This technique also allows the reconstruction of $\delta^{18}O_{sw}$, yielding information about the local hydrological cycle, an important aspect of climate which is mostly unconstrained in deep time. So far, the large sample sizes required for individual Δ_{47}-based temperature estimates (>2 mg) have complicated paleoseasonality reconstructions using this accurate method[22].

Here we combine clumped isotope analyses on microsampled (~100 µg) profiles through fossil bivalve shells with a novel statistical data reduction approach to obtain, for the first time, absolute SST and $\delta^{18}O_{sw}$ seasonality reconstructions of a greenhouse climate. We apply this new method to well-preserved oyster (*Rastellum diluvianum* and *Acutostrea incurva*) and rudist (*Biradiolites suecicus*) shells from Campanian (78.1±0.3 Ma[23]) coastal localities of the Kristianstad Basin in southern Sweden (46±3°N paleolatitude[24]; see **Fig. 1** and **METHODS**). We further supplement these reconstructions with results from fully coupled climate model simulations

of the Campanian greenhouse (see **METHODS**) to explore their implications for the "equable climate" hypothesis.

Results

All specimens showed clear seasonal $\delta^{18}O_c$ fluctuations of −2.0–0.0‰ in *R. diluvianum*, -2.0–0.0‰ in *A. incurva* and -2.7‰–-1.0‰ in *B. suecicus* on which shell chronologies were based (see **Methods**). These seasonal patterns show that the specimens record 3 (*A. incurva* and *B. suecicus*) to 6 (*R. diluvianum*) full years of growth. Clumped isotope analyses on small aliquots yielded Δ_{47} ranges between 0.62–0.73‰ for *R. diluvianum*, 0.64–0.76‰ for *A. incurva* and 0.63–0.75‰ for *B. suecicus*. Summaries of stable isotope measurement results are displayed in **Table 1**.

Detailed step-by-step results of the data processing routine are shown in **Supplementary Methods**. **Fig. 2** and **Table 1** show monthly Δ_{47}, SST and $\delta^{18}O_{sw}$ reconstructions for each specimen. Uncertainties at the 95% confidence level on monthly SST vary between 1.8 and 4.2°C owing to variable monthly sampling density related to intra-shell growth rate variability (**Fig. 2**). Statistically significant ($p<0.01$) SST seasonality was found in all specimens. Summer and winter temperatures, defined as mean temperatures of the warmest and coldest month, in *A. incurva* (13±2–26±4°C) and *B. suecicus* (14±4–25±3°C) are statistically indistinguishable ($p>0.2$), while SST from *R. diluvianum* are significantly higher (20±2–29±2°C; $p<0.05$). Significant $\delta^{18}O_{sw}$ seasonality was found in *R. diluvianum* (0.0±0.3–1.1±0.3‰VSMOW; $p<0.01$) and *B. suecicus* (-1.8±0.8–-0.6±0.5‰VSMOW; $p<0.01$), but not in *A. incurva* (-0.9±0.2–-0.4±0.9‰VSMOW; $p=0.07$; **Fig. 2**; **Table 1**). *R. diluvianum* records significantly higher $\delta^{18}O_{sw}$ values ($p<0.01$) than

the other specimens. In all specimens, monthly $\delta^{18}O_{sw}$ positively correlates with monthly SST (see **Fig. 2**).

Our climate model simulation yields global Campanian latitudinal gradients in summer, winter and Mean Annual Temperature (MAT; **Fig. 3A**) as well as monthly SST in the Boreal Chalk Sea (**Fig. 3B**). The modelled Campanian latitudinal SST gradient (24°C difference between tropics and high-latitude MAT) resembles the modern (25°C gradient). The global mean Campanian SST seasonality (8.2°C difference between warmest and coldest month) is similar to that in the modern ocean (8.6°C). Campanian global average SST at 4× preindustrial atmospheric pCO_2, however is ~22°C compared to ~14°C in the modern ocean (NOAA, 2020), yielding an equilibrium climate sensitivity, or global warming per doubling of atmospheric CO_2 concentration, of ~4°C[15]. Specifically, simulated SST at the Campanian Kristianstad Basin with 4× preindustrial atmospheric pCO_2 forcing (12±2–26±2°C seasonal range; **Fig. 3**) are much warmer than in present day southern Sweden (3±0.8–17±0.4°C[25]).

Discussion

Our novel Δ_{47}-based monthly SST and $\delta^{18}O_{sw}$ reconstructions from *A. incurva* and *B. suecicus* are statistically indistinguishable from model simulations of Campanian mid-latitude SST seasonality ($p>0.05$; **Fig. 3**). Higher SST (+4–5°C) and $\delta^{18}O_{sw}$ (+1.0–1.5‰) in *R. diluvianum* are due to the stronger seasonal insolation effect on its shallower (< 5 m) growth environment ($p<0.05$). By comparison, the deeper (5-15m) environment of *A. incurva* and *B. suecicus* was less affected by these processes and may have received more water with an open marine $\delta^{18}O_{sw}$ signature (closer to the -1‰VSMOW assumed for the ice-free Cretaceous; [26]Shackleton, 1986), especially in winter. These highly local differences are not resolved in the climate model simulations but show the unprecedented detail of SST and $\delta^{18}O_{sw}$ reconstructions the new clumped

isotope approach makes possible (see **Supplementary Discussion**). The ~1‰ higher $\delta^{18}O_{sw}$ in summer than in winter shows that summers in the Campanian Kristianstad Basin either experienced excess evaporation, which increases $\delta^{18}O_{sw}$ by preferentially removing isotopically light seawater, or less precipitation, which supplies isotopically light meteoric water, reducing $\delta^{18}O_{sw}$. Both processes lead to dry summers and wet winters compared to the annual average. The presence of growth stops cannot be fully excluded despite age model results suggesting none of the species stopped growing during a particular month of the year. A growth stop during extreme season (summer or winter) may cause slight underestimation of the full seasonal SST or $\delta^{18}O_{sw}$ range. Nevertheless, the remarkable agreement between Δ_{47}-based SST ranges and our climate model suggest that the average seasonal range reconstructed from all three specimens (15-27°C range, MAT of 20°C) likely represents the most accurate SST seasonality reconstructions for the Campanian Boreal Chalk Sea to date.

Strong seasonal fluctuations in $\delta^{18}O_{sw}$ (up to 1.3‰ in *B. suecicus*) and regular deviations from the commonly assumed -1‰VSMOW $\delta^{18}O_{sw}$ values[26] lead to large differences (up to 8.9°C in *R. diluvianum*) between SST estimates based on Δ_{47} and $\delta^{18}O_c$ (**Fig. 2**). The risk of assuming constant $\delta^{18}O_{sw}$ is even more clearly illustrated by significantly (+3.5–6.0°C) higher $\delta^{18}O_c$-based seasonal temperature reconstructions for *B. suecicus* compared to *A. incurva*, while both specimens grew under similar SST seasonality conditions (**Fig. 2B**). Similarly, $\delta^{18}O_c$-based temperature reconstructions of *A. incurva* and *R. diluvianum* are indistinguishable, while the paleoenvironment of *R. diluvianum* was at least 3.5°C warmer year-round (**Fig. 2B**), illustrating that the constant $\delta^{18}O_{sw}$ assumption is only valid in settings with negligible $\delta^{18}O_{sw}$ seasonality. Low-latitude Tethyan SST seasonality reconstructions based on rudist $\delta^{18}O_c$[10] agree with model simulations, which may indicate that the constant open ocean $\delta^{18}O_{sw}$ assumption may hold in these

environments, although data–model agreement is by no means solid evidence for correct $\delta^{18}O_{sw}$ assumptions and these should always be independently verified (**Fig. 3A**). A cold bias of ~8°C in $\delta^{18}O_c$-based SST reconstructions due to inaccurate $\delta^{18}O_{sw}$ assumptions was previously documented through the Δ_{47} method and proxy comparison[8,27], however this does not account for seasonal biases in the proxies.

Seasonal variability in growth rates in all specimens (**Fig 2A**) illustrates how bulk sampling of bio-archives can lead to significant biases in MAT reconstructions compared to our more accurate estimates of MAT as an average of monthly SST. In this case, slower summer and autumn growth (months 4-7 in **Fig. 2A**), especially in *A. incurva* and *B. suecicus*, would cause bulk analysis of shell material to underestimate MAT. Indeed, our Campanian mid-latitude SST ranges (~15-27°C, MAT of 20°C) are significantly higher than previous reconstructions of the same paleolatitude based on fish tooth $\delta^{18}O_c$ (15–20°C[11]), chalk $\delta^{18}O_c$ (12–15°C[12]), bulk mollusk Δ_{47} (5–12°C[28]), TEX_{86} (15–20°C[8]) and sub-annual mollusk $\delta^{18}O_c$ (15–22°C[10,23]; **Fig. 3A**). Given the increase in frequency and duration of growth stops in modern mollusks with increasing latitude[29], seasonal biases are likely more common in higher latitude environments. These two biases highlight the unique advantage of monthly resolved Δ_{47} records in eliminating the uncertainties of both unresolved seasonal variability and assumptions of constant $\delta^{18}O_{sw}$ on SST reconstructions.

Our robust data–model agreement down to the monthly scale provides strong evidence for considerably warmer (~8°C) higher latitudes during the Late Cretaceous greenhouse compared to the modern ocean. Previously heavily utilized shallow marine bio-archives from these latitudes are likely much more sensitive to $\delta^{18}O_{sw}$ and seasonality bias than low-latitude records. Such biases in previous reconstructions of greenhouse climates likely entail that the notion of greenhouse climates with shallow latitudinal temperature gradients are flawed, and that the Campanian

latitudinal temperature gradient resembled that of today. These results concur with the recent trend of converging data and model reconstructions yielding modern-scale Late Cretaceous latitudinal temperature gradients[13] and challenge the hypothesis of "equable climate" during all greenhouse periods[9]. Future work should see the accuracy of this latitudinal gradient estimate independently verified by applying the clumped isotope seasonality method on bivalve specimens from a range of latitudes in greenhouse climate periods. Moreover, these unique absolute monthly SST reconstructions corroborate growing evidence against the hypothesis of reduced temperature seasonality in greenhouse climates[30]. Results from *B. suecicus* represent the first Δ_{47}-based SST reconstructions from rudist bivalves, opening up an abundant archive for accurate Mesozoic SST seasonality reconstructions.

Conclusions

Our results merit re-evaluation of classical paleoclimate records that risk bias, such as those based on $\delta^{18}O_c$ (assuming constant $\delta^{18}O_{sw}$[7,10]), bulk analyses of macrofossils with growth seasonality (e.g. mollusks and brachiopods[31]) or microfossils with a fixed growth season (e.g. planktic foraminifera[32]) and organic proxies that may be seasonally biased (e.g. TEX_{86} and $U_{37}^{K'}$ [5,33]). In addition, monthly $\delta^{18}O_{sw}$ reconstructions allow, for the first time, the evaluation of local seasonality in the hydrological cycle from shallow marine bio-archives and climate models and reveal that summers were drier than winters in the Campanian Kristianstad Basin. This unique advantage of Δ_{47}-based seasonality reconstructions enables the reconstruction of previously unknown high-resolution variability in salinity, local rainfall and evaporation in past climates. Combined with longer-term, global-scale paleoclimate records, our new method for absolute monthly SST and $\delta^{18}O_{sw}$ reconstructions has the potential to resolve critical disagreements between SST proxies, reduce biases of deep-time paleoclimate reconstructions, shed light on new

aspects of past climate seasonality and reconcile proxy reconstructions and model simulations of greenhouse climate.

MAIN REFERENCES

1. Marshall, D. J. & Burgess, S. C. Deconstructing environmental predictability: seasonality, environmental colour and the biogeography of marine life histories. *Ecology Letters* **18**, 174–181 (2015).
2. Matthews, T., Mullan, D., Wilby, R. L., Broderick, C. & Murphy, C. Past and future climate change in the context of memorable seasonal extremes. *Climate Risk Management* **11**, 37–52 (2016).
3. Carré, M. & Cheddadi, R. Seasonality in long-term climate change. *Quaternaire. Revue de l'Association française pour l'étude du Quaternaire* 173–177 (2017) doi:10.4000/quaternaire.8018.
4. Zeebe, R. E., Zachos, J. C. & Dickens, G. R. Carbon dioxide forcing alone insufficient to explain Palaeocene–Eocene Thermal Maximum warming. *Nature Geoscience* **2**, 576 (2009).
5. Cramwinckel, M. J. *et al.* Synchronous tropical and polar temperature evolution in the Eocene. *Nature* **559**, 382 (2018).
6. IPCC. *IPCC, 2013: Climate Change 2013: The Physical Science Basis. Contribution of Working Group I to the Fifth Assessment Report of the Intergovernmental Panel on Climate Change, 1535 pp*. (Cambridge Univ. Press, Cambridge, UK, and New York, 2013).
7. Jenkyns, H. C., Forster, A., Schouten, S. & Damsté, J. S. S. High temperatures in the late Cretaceous Arctic Ocean. *Nature* **432**, 888 (2004).

8. O'Brien, C. L. *et al.* Cretaceous sea-surface temperature evolution: Constraints from TEX 86 and planktonic foraminiferal oxygen isotopes. *Earth-Science Reviews* **172**, 224–247 (2017).
9. Huber, B. T., Hodell, D. A. & Hamilton, C. P. Middle–Late Cretaceous climate of the southern high latitudes: stable isotopic evidence for minimal equator-to-pole thermal gradients. *Geological Society of America Bulletin* **107**, 1164–1191 (1995).
10. Steuber, T., Rauch, M., Masse, J.-P., Graaf, J. & Malkoč, M. Low-latitude seasonality of Cretaceous temperatures in warm and cold episodes. *Nature* **437**, 1341–1344 (2005).
11. Pucéat, E. *et al.* Fish tooth δ18O revising Late Cretaceous meridional upper ocean water temperature gradients. *Geol* **35**, 107 (2007).
12. Thibault, N., Harlou, R., Schovsbo, N. H., Stemmerik, L. & Surlyk, F. Late Cretaceous (late Campanian–Maastrichtian) sea-surface temperature record of the Boreal Chalk Sea. *Climate of the Past* **12**, 429–438 (2016).
13. Upchurch Jr, G. R., Kiehl, J., Shields, C., Scherer, J. & Scotese, C. Latitudinal temperature gradients and high-latitude temperatures during the latest Cretaceous: Congruence of geologic data and climate models. *Geology* **43**, 683–686 (2015).
14. Farnsworth, A. *et al.* Climate Sensitivity on Geological Timescales Controlled by Nonlinear Feedbacks and Ocean Circulation. *Geophys. Res. Lett.* **46**, 9880–9889 (2019).
15. Joussaume, S. & Braconnot, P. Sensitivity of paleoclimate simulation results to season definitions. *Journal of Geophysical Research: Atmospheres* **102**, 1943–1956 (1997).
16. Mosbrugger, V. Nearest-living-relative method. *Encyclopedia of paleoclimatology and ancient environments* 607–609 (2009).
17. Kim, S.-T. & O'Neil, J. R. Equilibrium and nonequilibrium oxygen isotope effects in synthetic carbonates. *Geochimica et Cosmochimica Acta* **61**, 3461–3475 (1997).

18. Jaffrés, J. B. D., Shields, G. A. & Wallmann, K. The oxygen isotope evolution of seawater: A critical review of a long-standing controversy and an improved geological water cycle model for the past 3.4 billion years. *Earth-Science Reviews* **83**, 83–122 (2007).

19. Veizer, J. & Prokoph, A. Temperatures and oxygen isotopic composition of Phanerozoic oceans. *Earth-Science Reviews* **146**, 92–104 (2015).

20. Eiler, J. M. "Clumped-isotope" geochemistry—The study of naturally-occurring, multiply-substituted isotopologues. *Earth and Planetary Science Letters* **262**, 309–327 (2007).

21. Petersen, S. V. *et al.* Effects of Improved 17O Correction on Interlaboratory Agreement in Clumped Isotope Calibrations, Estimates of Mineral-Specific Offsets, and Temperature Dependence of Acid Digestion Fractionation. *Geochemistry, Geophysics, Geosystems* **20**, 3495–3519 (2019).

22. Fernandez, A. *et al.* A reassessment of the precision of carbonate clumped isotope measurements: implications for calibrations and paleoclimate reconstructions. *Geochemistry, Geophysics, Geosystems* **18**, 4375–4386 (2017).

23. de Winter, N. J. *et al.* Shell chemistry of the boreal Campanian bivalve *Rastellum diluvianum* (Linnaeus, 1767) reveals temperature seasonality, growth rates and life cycle of an extinct Cretaceous oyster. *Biogeosciences* **17**, 2897–2922 (2020).

24. Surlyk, F. & Sørensen, A. M. An early Campanian rocky shore at Ivö Klack, southern Sweden. *Cretaceous Research* **31**, 567–576 (2010).

25. NOAA Global Surface Temperature (NOAAGlobalTemp) data provided by the NOAA/OAR/ESRL PSL, Boulder, Colorado, USA, https://psl.noaa.gov/, last accessed: 28/05/2020.

26. Shackleton, N. J. Paleogene stable isotope events. *Palaeogeography, Palaeoclimatology, Palaeoecology* **57**, 91–102 (1986).

27. Tagliavento, M., John, C. M. & Stemmerik, L. Tropical temperature in the Maastrichtian Danish Basin: Data from coccolith Δ47 and δ18O. *Geology* **47**, 1074–1078 (2019).

28. Petersen, S. V. *et al.* Temperature and salinity of the Late Cretaceous western interior seaway. *Geology* **44**, 903–906 (2016).

29. Lartaud, F. *et al.* A latitudinal gradient of seasonal temperature variation recorded in oyster shells from the coastal waters of France and The Netherlands. *Facies* **56**, 13 (2009).

30. Burgener, L., Hyland, E., Huntington, K. W., Kelson, J. R. & Sewall, J. O. Revisiting the equable climate problem during the Late Cretaceous greenhouse using paleosol carbonate clumped isotope temperatures from the Campanian of the Western Interior Basin, USA. *Palaeogeography, Palaeoclimatology, Palaeoecology* **516**, 244–267 (2019).

31. Henkes, G. A. *et al.* Temperature evolution and the oxygen isotope composition of Phanerozoic oceans from carbonate clumped isotope thermometry. *Earth and Planetary Science Letters* **490**, 40–50 (2018).

32. Pearson, P. N. *et al.* Warm tropical sea surface temperatures in the Late Cretaceous and Eocene epochs. *Nature* **413**, 481–487 (2001).

33. Jia, G., Wang, X., Guo, W. & Dong, L. Seasonal distribution of archaeal lipids in surface water and its constraint on their sources and the TEX86 temperature proxy in sediments of the South China Sea. *Journal of Geophysical Research: Biogeosciences* **122**, 592–606 (2017).

Table 1: Overview of analytical results ($\delta^{18}O_c$ and Δ_{47}) and reconstructions

Species (locality)	age [yr]	Measurement results: $\delta^{18}O_c$ [‰VPDB]				Δ_{47} [‰]				Monthly reconstructions: $\delta^{18}O_{sw}$ [‰VSMOW]			SST [°C]		
		N [b]	*min.*	*mean*	*max*	*N*	*min.*	*mean*	*max*	*CM* [c]	*MA* [d]	*WM* [e]	*CM*	*MA*	*WM*
R. diluvianum **(Ivö Klack)**	6.2	198	**-2.08** *±0.08*	**-1.16** *±0.08*	**0.18** *±0.08*	121	**0.605** *±0.077*	**0.678** *±0.077*	**0.795** *±0.077*	**0.00** *±0.27*	**0.56** *±0.11*	**1.08** *±0.36*	**19.6** *±1.8*	**24.6** *±0.7*	**29.2** *±2.3*
A. incurva **(Åsen)**	3.3	150	**-2.26** *±0.08*	**-0.71** *±0.08*	**0.15** *±0.08*	115	**0.601** *±0.077*	**0.706** *±0.077*	**0.831** *±0.077*	**-0.89** *±0.18*	**-0.46** *±0.09*	**-0.36** *±0.87*	**12.7** *±2.3*	**16.4** *±0.7*	**25.7** *±4.2*
B. suecicus **(Maltesholm)**	3	178	**-2.93** *±0.08*	**-1.99** *±0.08*	**-0.98** *±0.08*	102	**0.565** *±0.077*	**0.688** *±0.077*	**0.779** *±0.077*	**-1.81** *±0.78*	**-1.18** *±0.17*	**-0.55** *±0.45*	**13.7** *±3.9*	**19.3** *±0.9*	**24.8** *±2.6*

N = Number of measurements and the age is estimated from the age modelling results (**Supplementary Data 1**), CM = Coldest Month, MA = Mean Annual, WM = Warmest Month. All uncertainties are given as 95% confidence levels.

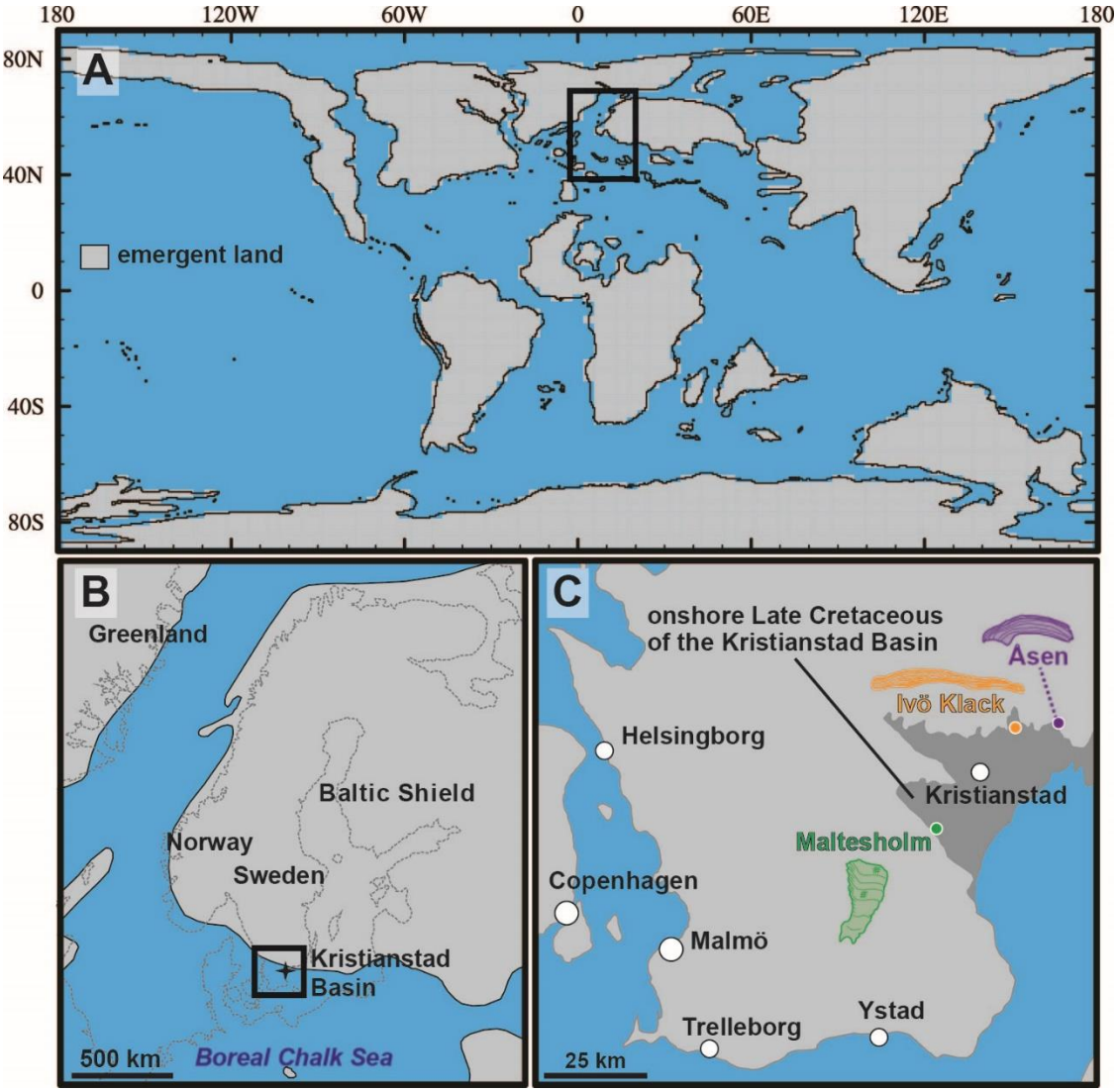

279

280 **Fig. 1**: **Campanian (78 Ma) paleogeography and geological setting A**) Global paleogeography
281 used in climate model[14] **B**) Northern Europe, black star indicates the Kristianstad Basin **C**)
282 Southern Sweden with Kristianstad Basin (submerged in the Campanian). Colored dots indicate
283 the three sampled localities on the paleoshoreline with schematic representations of the species. In
284 all maps, blue color indicates sea surface and light grey indicates emergent land. Maps **B**) and **C**)
285 are adapted from[34].

286

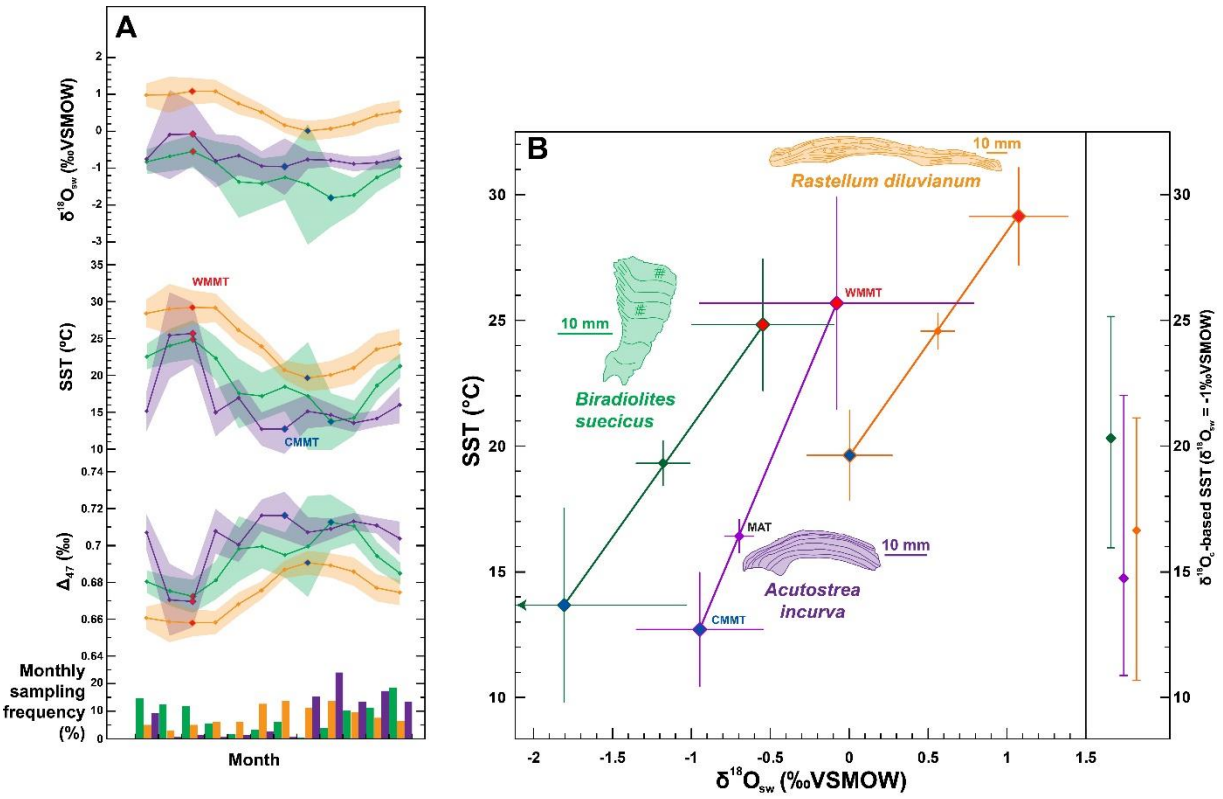

287

288 **Fig. 2**: **Paleoseasonality reconstructions A**) From bottom to top: relative monthly sampling
289 frequencies (bar chart), monthly average Δ_{47}, SST and $\delta^{18}O_{sw}$ reconstructions from *R. diluvianum*
290 (orange), *A. incurva* (purple) and *B. suecicus* (green). Shaded envelopes indicate 95% confidence
291 levels. Red and blue dots respectively indicate warmest and coldest months. **B**) SST and $\delta^{18}O_{sw}$
292 reconstructions of warmest month (red symbols), coldest month (blue symbols) and annual average
293 (symbols in color of specimen). Thin crosses indicate 95% confidence level uncertainties. Vertical
294 bars on the right indicate summer, winter and MAT estimates from $\delta^{18}O_c$ (assuming constant
295 $\delta^{18}O_{sw}$ of -1‰VSMOW). Scaled cross-sections through specimens are drawn with horizontal 10
296 mm scale bars.

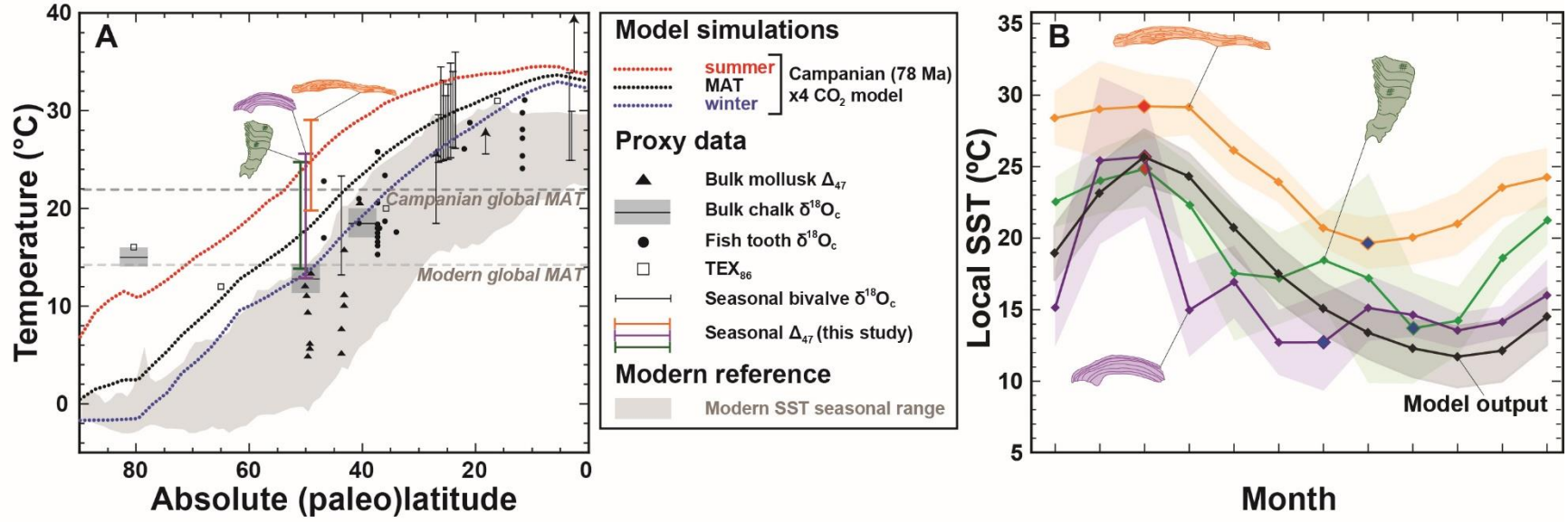

Fig. 3: **Comparison between model and reconstructions**. **A**) Campanian latitudinal SST gradient with vertical orange, purple and green bars showing seasonality reconstructions and dashed red, blue and black lines indicating modeled summer (warmest month), winter (coldest month) and mean annual temperatures respectively. Black symbols and bars show previous SST reconstructions[7,8,10,11,12,28,35,36]. The shaded grey envelope indicates modern seasonal SST range[25]. Horizontal dashed lines mark modern and Campanian global MAT. **B**) Monthly SST reconstructions (in orange, purple and green) and local model output (in black) in the Boreal Chalk Sea. Shaded envelopes show 95% confidence levels and color coding follows **Fig. 2**.

METHODS

Geological setting

The bivalve specimens used in this study originated from the Ivö Klack (*R. diluvianum*), Åsen (*A. incurva*) and Maltesholm (*B. suecicus*) localities in the Kristianstad Basin in southern Sweden (56°2’ N, 14° 9’ E; 46±3°N paleolatitude[24,37]; see **Fig. 1** and **Supplementary Data 7**). The three distinct localities contain a rich (> 200 species), well preserved Campanian rocky shore fauna[24,34] and were all deposited at the peak of transgression of the latest early Campanian, as supported by the restriction of these deposits to the *Belemnellocamax mammillatus* belemnite biozone and Sr-isotope chemostratigraphy[23,34,38]. The tectonic quiescence of the region since the Late Cretaceous limited burial and promoted excellent shell preservation[24]. The Kristianstad Basin represents the highest latitude location for the occurrence of rudist bivalves known to date[34].

Materials

Fossil *R. diluvianum* oysters were found *in situ* clinging to the sides of large boulders at a paleodepth of <5 m[24], while the *B. suecis* rudist and *A. incurva* oysters were found in a deeper setting (5–15m) among skeletal fragments on the paleo-seafloor[39]. Trace element (e.g. Sr/Ca and Mn/Ca) patterns and ultrastructure preservation demonstrate excellent preservation of primary calcite[23,39] (**Supplementary Methods**).

Sampling

Powdered samples (~300 µg) were drilled in growth direction from polished cross sections through the shell’s axis of maximum growth using a Dremel® 3000 rotary drill (Robert Bosch Ltd., Uxbridge, UK) equipped with a 300 µm wide tungsten carbide drill bit. High (~100 µm) sampling resolution was achieved by careful abrasive drilling using the side of the drill parallel to the growth

lines in the shell. In oyster shells, the well-preserved foliated calcite was targeted, while in the rudist the dense outer calcite was sampled, avoiding the honeycomb structure in the inner part of the outer shell layer which is more susceptible to recrystallization[40]. A total of 145 samples was obtained, from which 338 aliquots of ~100 µg were analyzed (see **Table 1**).

Clumped isotope analyses

Clumped isotope (Δ_{47}) analyses were carried out on Thermo Fisher Scientific MAT253 and 253 Plus mass spectrometers coupled to a Kiel IV carbonate preparation devices. Calcite samples (individual replicates of ~90 µg for MAT253 Plus and ~150 µg for MAT253) were reacted at 70 °C with nominally anhydrous (103%) phosphoric acid. The resulting CO_2 gas was cleaned from water and organic compounds with two cryogenic LN2 traps and a PoraPak Q trap kept at −40 °C. The purified sample gases were analyzed in micro-volume LIDI mode with 400 s integration time against a clean CO_2 working gas ($\delta^{13}C$ = -2.82‰; $\delta^{18}O$ = -4.67‰), corrected for the pressure baseline[41,42] and converted into the absolute reference frame by creating and empirical transfer function from the daily analyzed ETH calcite standards (ETH-1, -2, -3) and their accepted values[43]. All isotope data were calculated using the new IUPAC parameters following [44] and Δ_{47} values were projected to a 25 °C acid reaction temperature with a correction factor of 0.062 ‰[45,46]. Long-term Δ_{47} reproducibility standard deviation was 0.04‰ based on repeated measurements of ~100 µg aliquots of our check standard IAEA C2 (Δ_{47} of 0.719‰; measured over a 20-month period; see **Supplementary Data 8** for details). For the $\delta^{18}O_c$ compositions we applied an acid correction factor of 1.00871[17] and reported versus VPDB with a typical reproducibility below 0.08‰ (95% confidence level). Results were combined with $\delta^{18}O_c$ data previously measured in the same

shells[23,39] (**Supplementary Data 2**) to improve the confidence of seasonal age models and the temporal resolution of SST and $\delta^{18}O_{sw}$ reconstructions.

Absolute paleoseasonality reconstructions

We reconstructed absolute SST seasonality by aligning Δ_{47} data relative to the seasonal cycle using an age modelling routine[47] (**Supplementary Data 1 and 9**). The number of 100 µg Δ_{47} aliquots to combine into monthly SST estimates is optimized by grouping aliquots from the same month in different growth years. Analytical uncertainties are propagated through this optimization procedure using Monte Carlo simulations (details in **Supplementary Methods** and **Supplementary Data 10**). SST's are calculated from Δ_{47} values in monthly time bins ($1/12^{th}$ of the seasonal cycle) using the temperature calibration by [48] recalculated in [43], and $\delta^{18}O_{sw}$ is reconstructed from Δ_{47}-SST and $\delta^{18}O_c$ following [17] (**Supplementary Methods** and **Supplementary Data 3**). Seasonality is defined as the difference between the average temperatures in the warmest and coldest month, while mean annual temperature (MAT) is expressed as the average of all monthly temperatures, following USGS definitions[49]. Statistical analyses of seasonality, differences between specimens and differences between data and model are summarized in **Supplementary Data 4**.

Climate model

We utilize a fully equilibrated (>11,000 model years) paleoclimate model (HadCM3L) Campanian (78 Ma) simulation. Model boundary conditions (topography, bathymetry, solar luminosity) for the Campanian are the same as in [14]. pCO_2 is set to 1120 ppmV, within the range of pCO_2 reconstructions compiled by [50] and a modern astronomical configuration with dynamic

vegetation. Local seasonal SSTs are calculated for the paleorotated Kristianstad Basin (42.5-50°N, 7.5-15°E; **Supplementary Data 5**). For comparison, modern SST data come from the National Oceanic and Atmospheric Administration[25] (**Supplementary Data 6**). See **Supplementary Methods** for further details.

Data availability

Extended methods, data and scripts belonging to this study are available in the open-access database Zenodo (https://doi.org/10.5281/zenodo.3865428).

METHODS REFERENCES

34. Sørensen, A. M., Surlyk, F. & Jagt, J. W. M. Adaptive morphologies and guild structure in a high-diversity bivalve fauna from an early Campanian rocky shore, Ivö Klack (Sweden). *Cretaceous Research* **33**, 21–41 (2012).
35. de Winter, N. J. *et al.* Tropical seasonality in the late Campanian (late Cretaceous): Comparison between multiproxy records from three bivalve taxa from Oman. *Palaeogeography, Palaeoclimatology, Palaeoecology* **485**, 740–760 (2017).
36. Walliser, E. O., Mertz-Kraus, R. & Schöne, B. R. The giant inoceramid Platyceramus platinus as a high-resolution paleoclimate archive for the Late Cretaceous of the Western Interior Seaway. *Cretaceous Research* **86**, 73–90 (2018).
37. van Hinsbergen, D. J. *et al.* A paleolatitude calculator for paleoclimate studies. *PloS one* **10**, e0126946 (2015).
38. Christensen, W. K. Paleobiogeography and migration in the Late Cretaceous belemnite family Belemnitellidae. *Acta palaeontologica polonica* **42**, 457–495 (1997).

39. Sørensen, A. M., Ullmann, C. V., Thibault, N. & Korte, C. Geochemical signatures of the early Campanian belemnite Belemnellocamax mammillatus from the Kristianstad Basin in Scania, Sweden. *Palaeogeography, palaeoclimatology, palaeoecology* **433**, 191–200 (2015).
40. Pons, J. M. & Vicens, E. The structure of the outer shell layer in radiolitid rudists, a morphoconstructional approach. *Lethaia* **41**, 219–234 (2008).
41. Bernasconi, S. M. *et al.* Background effects on Faraday collectors in gas-source mass spectrometry and implications for clumped isotope measurements. *Rapid Communications in Mass Spectrometry* **27**, 603–612 (2013).
42. Meckler, A. N., Ziegler, M., Millán, M. I., Breitenbach, S. F. & Bernasconi, S. M. Long-term performance of the Kiel carbonate device with a new correction scheme for clumped isotope measurements. *Rapid Communications in Mass Spectrometry* **28**, 1705–1715 (2014).
43. Bernasconi, S. M. *et al.* Reducing uncertainties in carbonate clumped isotope analysis through consistent carbonate-based standardization. *Geochemistry, Geophysics, Geosystems* **19**, 2895–2914 (2018).
44. Daëron, M., Blamart, D., Peral, M. & Affek, H. P. Absolute isotopic abundance ratios and the accuracy of Δ47 measurements. *Chemical Geology* **442**, 83–96 (2016).
45. Defliese, W. F., Hren, M. T. & Lohmann, K. C. Compositional and temperature effects of phosphoric acid fractionation on Δ47 analysis and implications for discrepant calibrations. *Chemical Geology* **396**, 51–60 (2015).
46. Murray, S. T., Arienzo, M. M. & Swart, P. K. Determining the Δ47 acid fractionation in dolomites. *Geochimica et Cosmochimica Acta* **174**, 42–53 (2016).

47. Judd, E. J., Wilkinson, B. H. & Ivany, L. C. The life and time of clams: Derivation of intra-annual growth rates from high-resolution oxygen isotope profiles. *Palaeogeography, Palaeoclimatology, Palaeoecology* **490**, 70–83 (2018).
48. Kele, S. *et al.* Temperature dependence of oxygen-and clumped isotope fractionation in carbonates: a study of travertines and tufas in the 6–95 C temperature range. *Geochimica et Cosmochimica Acta* **168**, 172–192 (2015).
49. O'Donnell, M. S. & Ignizio, D. A. Bioclimatic predictors for supporting ecological applications in the conterminous United States. *US Geological Survey Data Series* **691**, (2012).
50. Foster, G. L., Royer, D. L. & Lunt, D. J. Future climate forcing potentially without precedent in the last 420 million years. *Nature Communications* **8**, 14845 (2017).

ACKNOWLEDGEMENTS

NJW is funded by the Flemish Research Council (FWO; junior postdoc grant; 12ZB220N) and the European Commission (MSCA Individual Fellowship; UNBIAS project 843011). NT acknowledges Carslbergfondet CF16-0457. PC would like to acknowledge funding from the VUB Strategic Research grant (internal). The authors would like to thank Bart Lippens for help with sample preparation, Arnold van Dijk for analytical support and Anne Sørensen for helping out with sample collection.

AUTHOR CONTRIBUTIONS

The initial design of the study was conceived by NJW, NT, CVU and MZ. NJW, IAM, IJK and MZ together were responsible for clumped isotope data acquisition. NT and CVU provided

samples used in this study. DJL and AF ran the climate model and provided in-depth input on model-data integration. NJW and PC were responsible for acquiring the funding needed for this study. NJW wrote the first draft of the manuscript. All authors then contributed to the writing process.

COMPETING INTEREST DECLARATION

The authors have no competing interest to declare.

SUPPLEMENTARY INFORMATION

All supplementary material belonging to this manuscript is deposited in the open-source online database Zenodo (https://doi.org/10.5281/zenodo.3865428).